Supplement

eMethods

PET-based staging systems

PET-based staging systems were included as non-binary categorical measures of Aβ and tau pathology. We included two systems for Aβ: a three-stage system developed by Mattsson et al[1] and a four-stage system developed by Collij et al[2]. We included Braak staging for tau[3,4], including both a three-stage and six-stage version. Each stage in each system was associated with a collection of Freesurfer ROIs (stage composite), as shown in eTable 2, with advancing stages indicating regions where pathology spreads over the disease course.

The method for Mattsson staging and Braak staging were similar and proceeded as follows. First, an average SUVR was calculated in each stage composite using a volume weighted average of bilateral regions. Next, Gaussian mixture models (GMM) were fit to the distribution of uptake in each stage composite to estimate a binary cutoff for stage positivity (as described in the main text Methods: Image-based biomarker definitions). These cutoffs allowed us to assign binary positivity measures for each subject in each stage composite. Disease stages were then assigned based on individual patterns of positivity: to be assigned a given disease stage, an individual had to exhibit positivity for that stage and all prior ones. In case an individual was positive for a given stage but not all prior stages, they were marked as non-stageable. Individuals could also be assigned stage 0 if they were not positive for pathology in any stage composite.

Collij staging was slightly different in that positivity for a stage composite was based on being positive for pathology in most ROIs corresponding to a given stage. That is, GMMs were fit to each Freesurfer ROI individually, and positivity for a stage composite was defined by exhibiting supra-threshold uptake in 50% or more of the

associated ROIs. Disease stage assignment then proceeded in the same manner as for Mattsson and Braak staging (individuals needed to be positive for a given disease stage and all prior stages).

Cross-validation experiments

Cross-validated modeling was implemented in Python (v3.10) using scikit-learn (v1.4.2). For all cross-validation experiments, CDR status was used as a stratifying variable. Random samples were also seeded, such that the individuals of each testing fold were the same across experiments with the same input data. All cross-validation experiments had 10 outer folds and were repeated 10 times to generate 100 out of sample error estimates for each tested model.

We first ran models for each biomarker separately to assess the predictive value of each included definition. These experiments used a non-nested, 10-fold cross-validation. In each iteration, training data were used to fit linear regressions where PHC_{Global} was predicted from a single biomarker and covariates (age, sex, *APOE* E4 positivity). That is, separate models were fit for each biomarker. Biomarker definitions with tunable parameters (Z-scores, GMMs) were also fit with training data. A baseline model was also trained in each iteration which only included covariates as predictors. Trained models were then evaluated on the testing fold data, and the prediction accuracies for each were calculated as root mean squared error (RMSE).

We next created combinatorial models to test if combination of biomarkers improved prediction accuracy and if models incorporating continuous or non-categorical binary biomarkers outperformed models with binary biomarkers. For these experiments, we used nested cross-validation with 10 outer folds and 5 inner folds. In the inner cross-validation, a model selection procedure was applied to identify the best performing individual predictors (like the non-nested cross-validation experiment described above). Inner training data were used to fit linear models predicting PHC_{Global} with single biomarkers plus covariates as predictors. Inner testing data were used to measure the out-of-sample accuracy of these models. We then grouped the models based on the pathology (AT(N)) and variable type (binary/non-binary

categorical/continuous) and selected the best performing biomarker definitions (lowest average RMSE across 5 test folds). The outer cross-validation was then used for training new linear models which combined the biomarkers selected from the inner cross-validation. eTable 3 shows all the combinatorial linear models that were evaluated in the outer loop using this training scheme.

We also used support vector machine (SVM) regression to directly predict PHC_{Global} from imaging data. SVMs were trained using regional Aβ uptakes, tau uptakes, or gray matter volumes as input features. An additional model combined all these regional imaging features into a multimodal predictive model. SVM training used a nested cross-validation design with 10 outer folds and 5 inner folds. The inner loop was used for hyperparameter tuning for the regularization parameter C, the kernel, and the kernel coefficient γ. Search spaces were informed by consensus recommendations[5] and from pilot experiments: kernel (linear or radial basis function [RBF]), C with linear kernel $(2^{-10}, 2^{-9}, \cdots, 2^{-1}, 2^{0})$, C with RBF kernel $(2^{-5}, 2^{-3}, \cdots, 2^{13}, 2^{15})$, γ with RBF kernel $(2^{-15}, 2^{-13}, \cdots, 2^{1}, 2^{3})$. The best hyperparameters were determined from the inner loop (lowest average RMSE across 5 test folds) and used to retrain and evaluate SVM models in the outer loop.

Feature importance analyses

We ran additional post-hoc analyses to probe feature importance for our cross-validated linear modeling. For models which applied a model selection to filter biomarker definitions, we created pie charts showing the specific biomarker definitions which were selected as the best performing over repeated cross-validation iterations. We also extracted and plotted the (standardized) linear model coefficients for the Aβ, tau, and neurodegeneration biomarkers in all binary and all continuous models (non-binary categorical models were omitted because coefficient interpretation is less straightforward for non-binary categorical features). Finally, we visualized the cutoff values that were selected for Aβ and tau from models with all binary definitions.

For SVM models, we visualized the feature importance of individual brain regions for Aβ, tau, and neurodegeneration features. Following previous work[6,7], feature

85 importance values were generated by calculating the covariance of each feature and
86 PHC_{Global}. We generated brain maps showing the average feature importance across
87 100 out-of-sample model predictions. Maps were generated for the combined SVM and
88 for each unimodal SVM.

89

eTables

Name	Pathology	Variable type	Description
Aβ composite	Aβ	Continuous	Aβ SUVR in summary composite region
Centiloid	Aβ	Continuous	Linear transformation of Aβ composite SUVR[8]
Aβ SUVR>1.11	Aβ	Binary	Cutoff from Landau et al.[9]
Aβ SUVR>1.24	Aβ	Binary	Cutoff from Su et al.[10]
Aβ SUVR>1.42	Aβ	Binary	Cutoff from Jack et al.[11] (reliable worsening)
Aβ SUVR>1.30	Aβ	Binary	Cutoff from Jack et al.[11] (specificity)
Centiloid>15	Aβ	Binary	Binary cutoff for Centiloid
Centiloid>20	Aβ	Binary	Binary cutoff for Centiloid
Centiloid>25	Aβ	Binary	Binary cutoff for Centiloid
Centiloid>30	Aβ	Binary	Binary cutoff for Centiloid
Aβ composite (GMM)	Aβ	Binary	Aβ composite SUVR binarized with a GMM
Aβ composite (z>2.0)	Aβ	Binary	Z-score cutoff of 2 for Aβ composite SUVR
Aβ composite (z>2.5)	Aβ	Binary	Z-score cutoff of 2.5 for Aβ composite SUVR
Aβ composite (Quartiles)	Aβ	Non-binary categorical	Quartiles of the Aβ composite SUVR
Centiloid (Quartiles)	Aβ	Non-binary categorical	Quartiles of Centiloid
Mattsson staging	Aβ	Non-binary categorical	Aβ –PET staging system[2]
Collij staging	Aβ	Non-binary categorical	Aβ –PET staging system[1]
Aβ composite (BIZ)	Aβ	Non-binary categorical	Binarization with an intermediate zone for Aβ composite
Centiloid (BIZ)	Aβ	Non-binary categorical	Binarization with an intermediate zone for Centiloid
MT tau SUVR	Tau	Continuous	Tau SUVR in meta-temporal composite region
Braak I SUVR	Tau	Continuous	Tau SUVR in Braak I composite region
Braak III/IV SUVR	Tau	Continuous	Tau SUVR in Braak III/IV composite region
Braak V/VI SUVR	Tau	Continuous	Tau SUVR in Braak V/VI composite region
MT tau (GMM)	Tau	Binary	Meta-temporal tau SUVR binarized with a GMM
MT tau (z>2.0)	Tau	Binary	Z-score cutoff of 2 for MT tau SUVR
MT tau (z>2.5)	Tau	Binary	Z-score cutoff of 2.5 for MT tau SUVR
Tau SUVR>1.20	Tau	Binary	Cutoff from Jack et al.[11] (sensitivity)
Tau SUVR>1.21	Tau	Binary	Cutoff from Jack et al.[11] (specificity)
Tau SUVR>1.23	Tau	Binary	Cutoff from Jack et al.[11] (accuracy-young)
Tau SUVR>1.33	Tau	Binary	Cutoff from Jack et al.[11] (accuracy-matched)
MT tau (Quartiles)	Tau	Non-binary categorical	Quartiles of MT tau SUVR
MT tau (BIZ)	Tau	Non-binary categorical	Binarization with an intermediate zone for MT tau SUVR

Braak staging (3)	Tau	Non-binary categorical	Braak staging based on 3 stage model (I, III/IV, V/VI)
Braak staging (3)	Tau	Non-binary categorical	Braak staging based on 6 stage model (I, III, V, V, VI)
Hippocampus	Neurodegen.	Continuous	Hippocampal volume
MT volume	Neurodegen.	Continuous	Volume of the MT composite region
Hippocampus (z<-2.0)	Neurodegen.	Binary	Z-score cutoff of 2.0 for hippocampal volume
Hippocampus (z<-2.5)	Neurodegen.	Binary	Z-score cutoff of 2.5 for hippocampal volume
MT volume (z<-2.0)	Neurodegen.	Binary	Z-score cutoff of 2.0 for MT volume
MT volume (z<-2.5)	Neurodegen.	Binary	Z-score cutoff of 2.5 for MT volume
Hippocampus (Quartiles)	Neurodegen.	Non-binary categorical	Quartiles of hippocampal volume
MT volume (Quartiles)	Neurodegen.	Non-binary categorical	Quartiles of MT volume

eTable 1. Listing of all image-based AT(N) biomarkers used in cognitive prediction models.

Name	Citation	Regions
Aβ composite	[12,13]	caudal middle frontal, lateral orbitofrontal, medial orbitofrontal, pars opercularis, pars orbitalis, pars triangularis, rostral middle frontal, superior frontal, frontal pole, caudal anterior cingulate, isthmus cingulate, posterior cingulate, rostral anterior cingulate, inferior parietal, precuneus, superior parietal, supramarginal, inferior temporal, middle temporal, superior temporal
MT	[11]	entorhinal, amygdala, fusiform, inferior temporal, middle temporal
Braak I	[14,15]	entorhinal
Braak III		parahippocampal, fusiform, lingual, amygdala
Braak IV		middle temporal, caudal anterior cingulate, rostral anterior cingulate, posterior cingulate, isthmus cingulate, insula, inferior temporal, temporal pole
Braak V		superior frontal, lateral orbitofrontal, medial orbitofrontal, frontal pole, caudal middle frontal, rostral middle frontal, pars opercularis, pars orbitalis, pars triangularis, lateral occipital, supramarginal, inferior parietal, superior temporal, superior parietal, precuneus, bank of the superior temporal sulcus, transverse temporal
Braak VI		pericalcarine, postcentral, cuneus, precentral, paracentral
Mattsson Early	[1]	precuneus, posterior cingulate, isthmus cingulate, insula, medial orbitofrontal, lateral orbitofrontal
Mattsson Intermediate		bank SSTS, caudal middle frontal, cuneus, frontal pole, fusiform, inferior parietal, inferior temporal, lateral occipital, middle temporal, parahippocampal, pars opercularis, pas orbitalis, pars triangularis, putamen, rostral anterior cingulate, rostral middle frontal, supramarginal
Mattsson Late		lingual, pericalcarine, paracentral, precentral, postcentral
Colllij 1	[2]	posterior cingulate, isthmus cingulate, anterior cingulate (caudal+rostral)
Collij 2		lateral orbitofrontal, paracentral, precuneus, medial orbitofrontal, inferior frontal (pars opercularis+pas orbitalis+pars triangularis)
Collij 3		insula, fusiform, precentral, inferior temporal, parahippocampal, collijinferiorfrontal, superior frontal, lingual, supramarginal, inferior parietal, cuneus, middle frontal (rostral+caudal)
Collij 4		lateral occipital, superior parietal, middle temporal, superior temporal, postcentral, entorhinal, frontal pole, temporal pole

eTable 2. List of Freesurfer regions used for composite regions. Citations are included for papers which defined these composites. For Collij stging composites, regions shown joined by plus signs are meta-ROIs constructed prior to averaging for the composite, as described in the original paper[2]. Aβ=amyloid-beta, MT=meta-temporal, ROI=region of interest.

Model	Aβ	Tau	Neurodegen
Baseline	-	-	-
A_{BIN}	Binary	-	-
T_{BIN}	-	Binary	-
N_{BIN}	-	-	Binary
A_{CAT}	Non-binary categorical	-	-
T_{CAT}	-	Non-binary categorical	-
N_{CAT}	-	-	Non-binary categorical
A_{CON}	Continuous	-	-
T_{CON}	-	Continuous	-
N_{CON}	-	-	Continuous
$A_{BIN}/T_{BIN}/N_{BIN}$	Binary	Binary	Binary
$A_{CAT}/T_{CAT}/N_{CAT}$	Non-binary categorical	Non-binary categorical	Non-binary categorical
$A_{CON}/T_{CON}/N_{CON}$	Continuous	Continuous	Continuous
$A_{CAT}/T_{BIN}/N_{BIN}$	Non-binary categorical	Binary	Binary
$A_{BIN}/T_{CAT}/N_{BIN}$	Binary	Non-binary categorical	Binary
$A_{BIN}/T_{BIN}/N_{CAT}$	Binary	Binary	Non-binary categorical
$A_{CON}/T_{BIN}/N_{BIN}$	Continuous	Binary	Binary
$A_{BIN}/T_{CON}/N_{BIN}$	Binary	Continuous	Binary
$A_{BIN}/T_{BIN}/N_{CON}$	Binary	Binary	Continuous

eTable 3. List of linear models predicting PHC_{Global} from AT(N) biomarkers. Models were trained with a nested-cross validation scheme where the inner loop was used to select the best performing biomarkers, after grouping by pathology (Aβ, tau, neurodegeneration) and variable type. BIN, CAT, and CON are used to represent binary, non-binary categorical, and continuous variables (respectively). Dashes are shown to indicate omission of the corresponding biomarker in the model. All models also had age, sex, and *APOE* E4 status included as covariates.

	CDR=0.0	CDR=0.5	CDR=1.0+	p-value
n	223	130	30	
Age	73.76 (7.07)	75.73 (8.32)	77.78 (8.48)	**0.005**
Sex (M/F)	96/127	75/55	16/14	**0.026**
***APOE* E4+**	79 (35.4%)	45 (34.6%)	13 (43.3%)	0.659
Centiloid	19.92 (35.65)	41.74 (54.70)	69.79 (48.77)	**<0.001**
PHC_{Global}	0.84 (0.36)	0.35 (0.46)	-0.47 (0.55)	**<0.001**

eTable 4: Characteristics for the subsample with longitudinal cognitive followup.

	CDR=0.0	CDR=0.5	CDR=1.0+	p-value
n	143	83	20	
Age	73.29 (7.50)	74.26 (8.31)	75.91 (9.34)	0.322
Sex (M/F)	59/94	54/29	10/10	**0.003**
***APOE* E4+**	49 (34.3%)	29 (34.9%)	12 (60.0%)	0.076
Centiloid	19.94 (38.52)	45.26 (55.40)	74.68 (48.25)	**<0.001**
PHC_{Global}	0.87 (0.35)	0.32 (0.50)	-0.27 (0.53)	**<0.001**

eTable 5: Characteristics for the subsample with imaging and CSF biomarker assessments.

eFigures

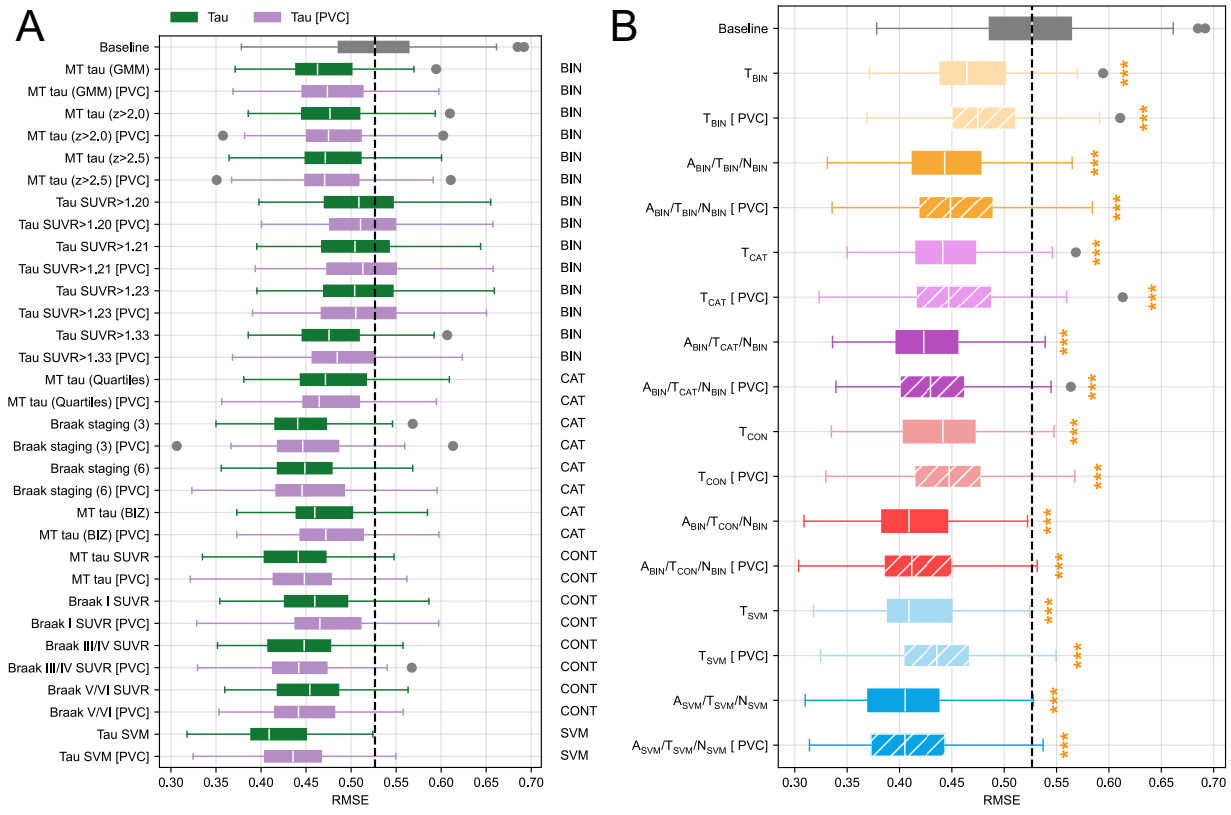

eFigure 1: Comparison of partial volume corrected (PVC) and non-PVC tau predictors for modeling cognition. **A.** Boxplots of cross-validated accuracy (RMSE) for models including a single tau predictor and covariates. **B.** Boxplots of cross-validated accuracy (RMSE) for models with the best selected tau predictors. Solid colors indicate models without tau PVC, while hatches indicate models with tau PVC. In both panels, the baseline model (just covariates) is shown in gray, with the dotted line indicating its mean performance. Gold stars indicate a significant improvement in accuracy relative to the baseline model (*p<0.05, **p<0.01, ***p<0.001). No significant differences were found for comparisons of PVC and non-PVC models (all p>0.05).

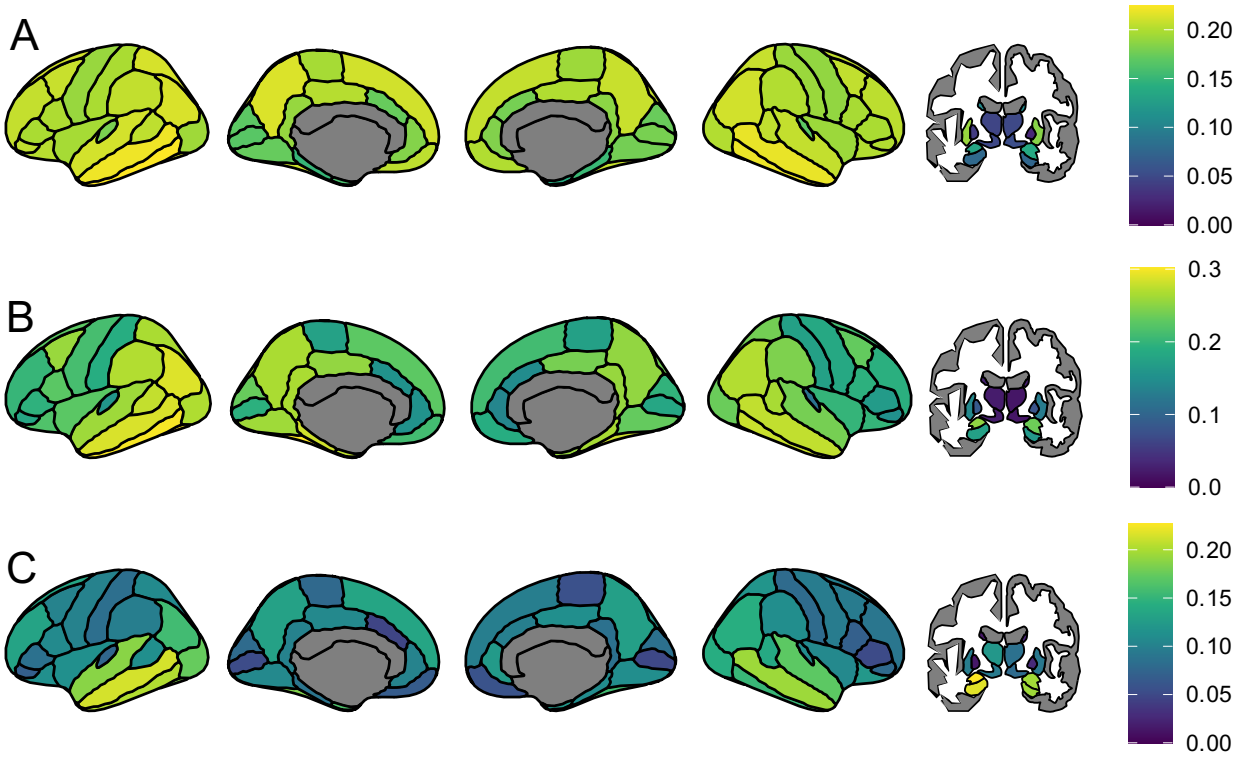

eFigure 2: Regional weights for SVM models which included only Aβ (**A,** A_{SVM}), tau (**B,** T_{SVM}), or gray matter volume (**C,** N_{SVM}).

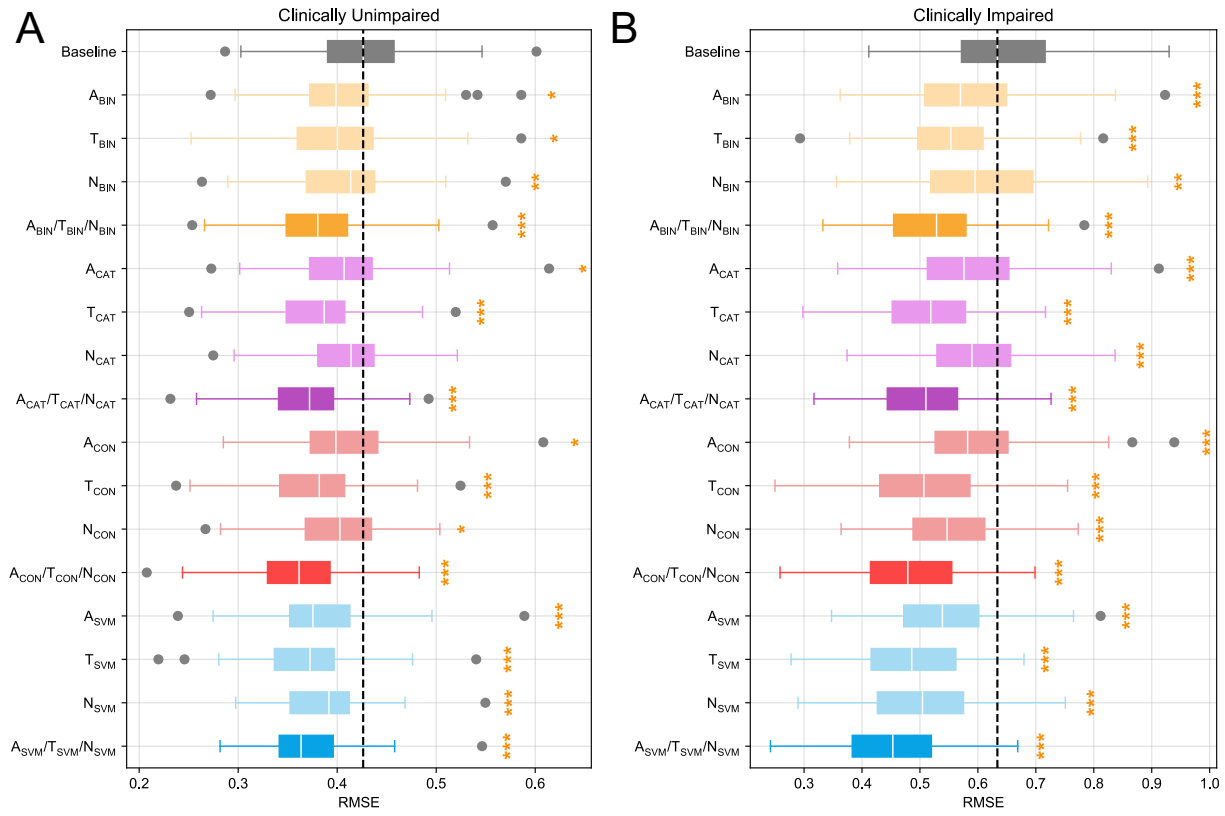

eFigure 3: Boxplots showing cross-validated accuracy (RMSE) measures for predicting PHC_{Global} in CU (**A**) and CI (**B**) individuals. Individual and combination biomarker models are compared against a baseline model using only covariates (mean performance indicated by dotted line) to predict PHC_{Global}. Colors are used to indicate the variable type of included biomarkers (yellow: binary, purple: non-binary categorical, red: continuous, blue: SVM). Lighter coloring indicates models which only have a single pathology assessment, while darker coloring indicates models which have Aβ, tau, and neurodegeneration biomarkers. Gold stars indicate a significant improvement in accuracy relative to the baseline model (*p<0.05, **p<0.01, ***p<0.001).

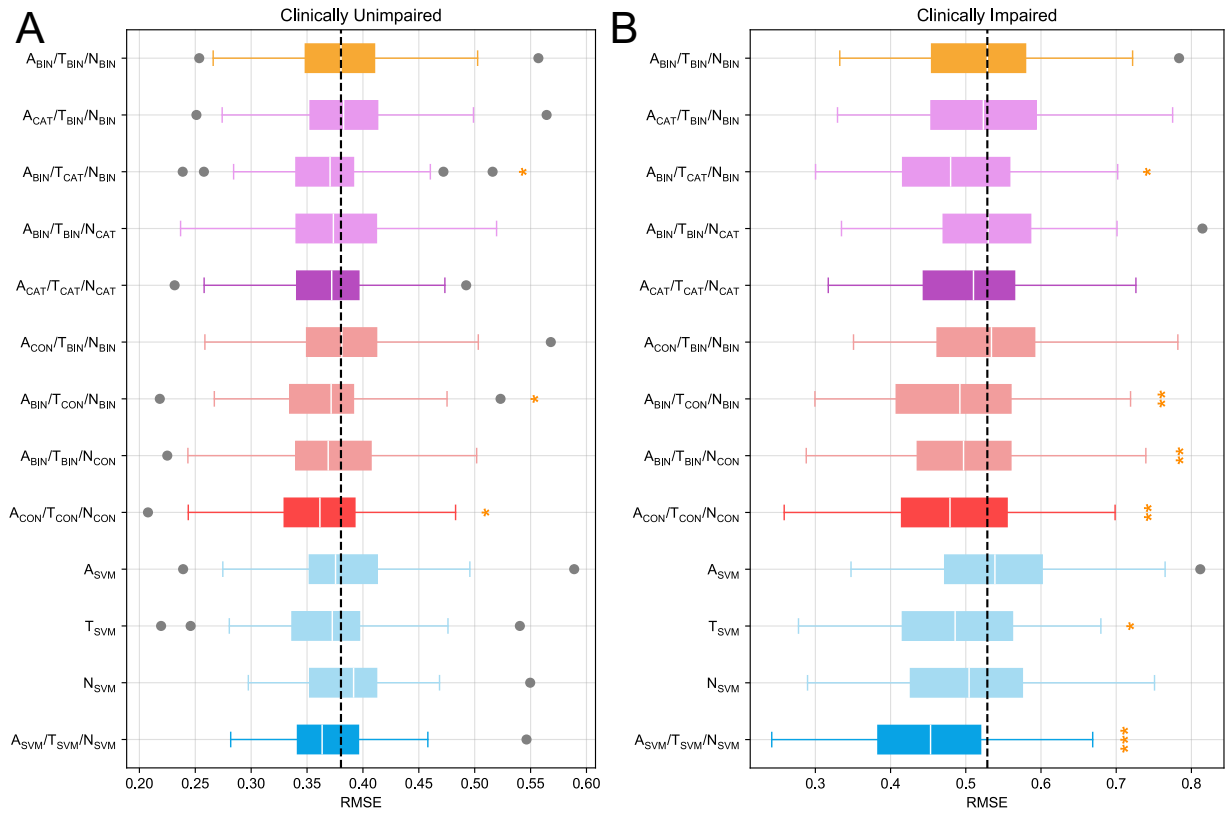

eFigure 4: Boxplots showing cross-validated accuracy (RMSE) measures for predicting PHC_{Global} in CU (**A**) and CI (**B**) individuals. Combination biomarker models with non-binary variable types are compared against a baseline model with binary biomarker definitions (mean performance indicated by dotted line). Colors are used to indicated the variable type of included biomarkers (yellow: binary, purple: non-binary categorical, red: continuous, blue: SVM). Lighter coloring indicates models which only have a single pathology assessment, while darker coloring indicates models which have Aβ, tau, and neurodegeneration biomarkers. Gold stars indicate a significant improvement in accuracy relative to the baseline model (*p<0.05, **p<0.01, ***p<0.001).

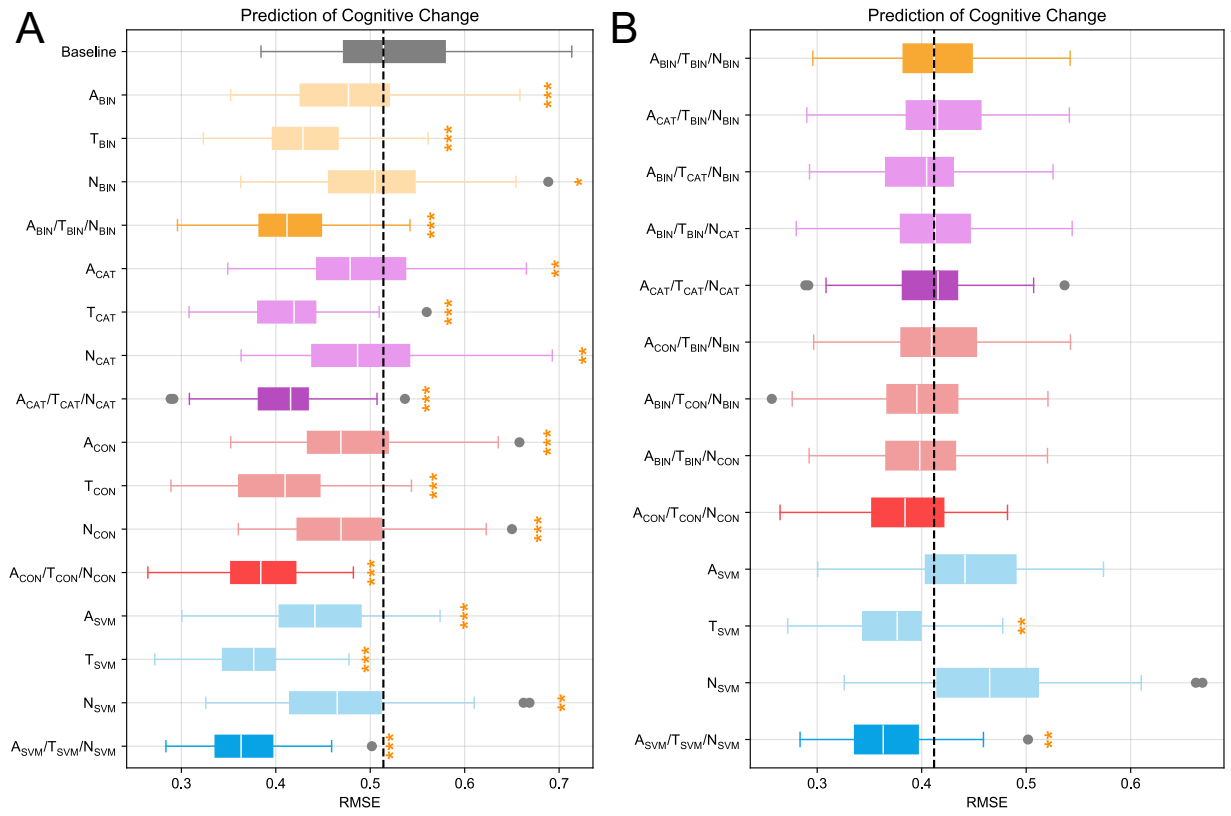

eFigure 5: Results from experiments predicting the longitudinal change in PHC_{Global}. **A.** Individual and combination biomarker models are compared against a baseline model using only covariates (mean performance indicated by dotted line). **B.** Combination biomarker models with non-binary variable types are compared against a baseline model with binary biomarker definitions (mean performance indicated by dotted line). In both panels, colors are used to indicate the variable type of included biomarkers (yellow: binary, purple: non-binary categorical, red: continuous, blue: SVM). Lighter coloring indicates models which only have a single pathology assessment, while darker coloring indicates models which have Aβ, tau, and neurodegeneration biomarkers. Gold stars indicate a significant improvement in accuracy relative to the topmost model. Gray stars and bars highlight significant pairwise differences between individual models. Statistical results are derived from Nadeau-Bengio t-tests with correction for multiple comparisons (*p<0.05, **p<0.01, ***p<0.001).

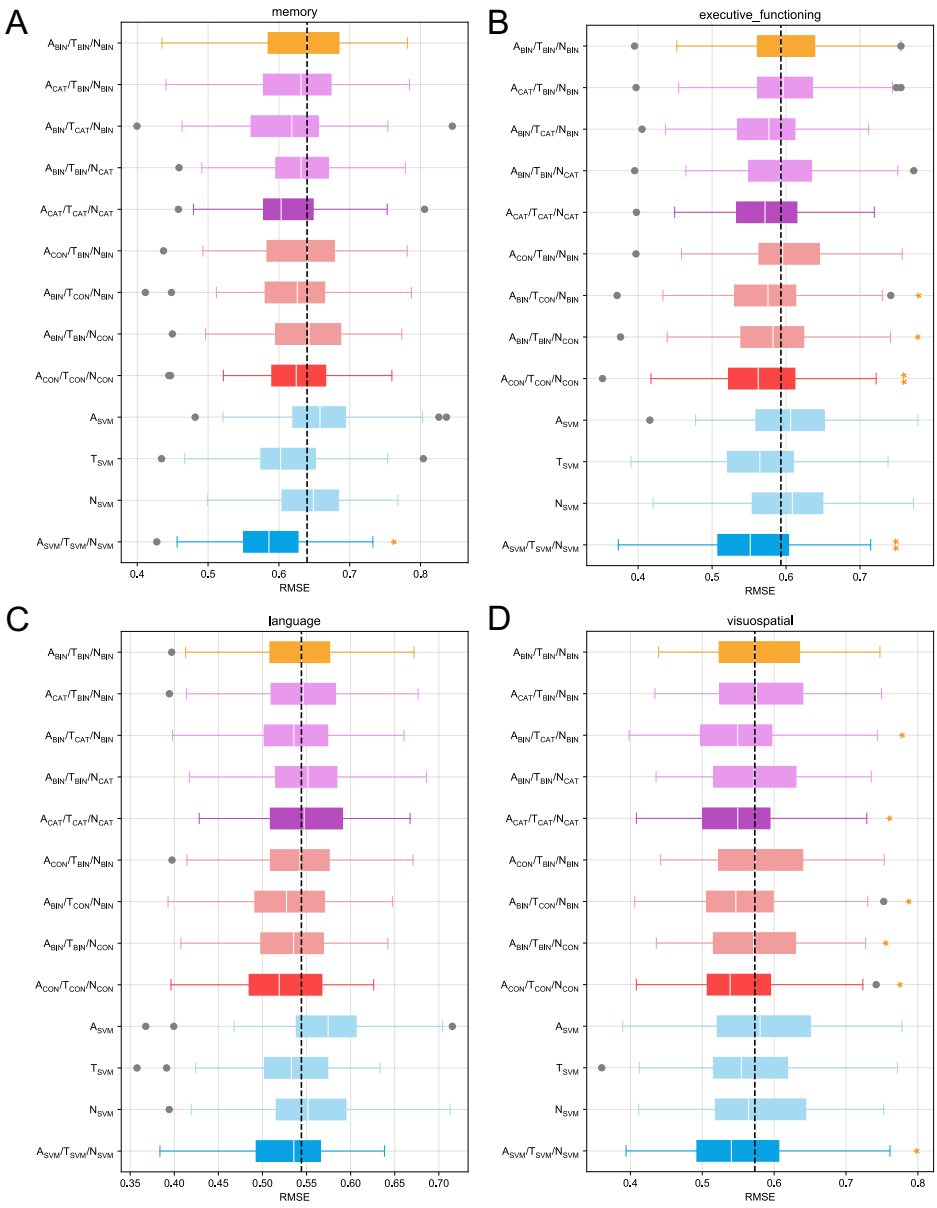

eFigure 6: Boxplots showing cross-validated accuracy estimates (RMSE) for models predicting neuropsychological performance from biomarkers. Panels show experiments using memory (A), executive functioning (B), language (C), and visuospatial (D) composites from the PHC as dependent variables. Combination biomarker models with non-binary variable types are compared against a baseline model with binary biomarker definitions (mean performance indicated by dotted line). In all panels, colors are used to indicate the variable type of included ATN biomarkers (yellow: binary, purple: non-binary categorical, red: continuous, blue: SVM). Lighter coloring indicates models which only have a single pathology assessment, while darker coloring indicates models which have Aβ, tau, and neurodegeneration biomarkers. Gold stars indicate a significant improvement in accuracy relative to the topmost model.

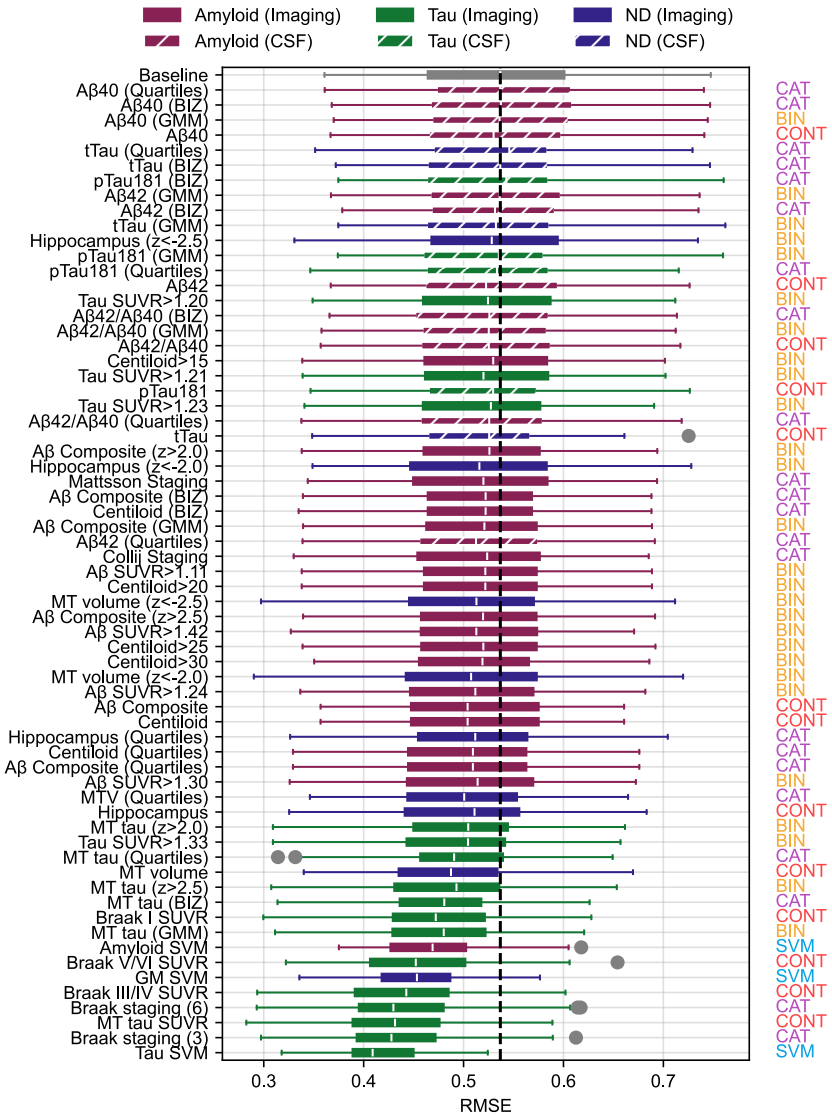

eFigure 7: Alternate version of main text Figure 1 including CSF predictors alongside imaging-based ones.

eReferences

1. Mattsson N, Palmqvist S, Stomrud E, Vogel J, Hansson O. Staging β-Amyloid Pathology With Amyloid Positron Emission Tomography. *JAMA Neurology*. 2019;76(11):1319-1329. doi:10.1001/jamaneurol.2019.2214

2. Collij LE, Heeman F, Salvadó G, et al. Multitracer model for staging cortical amyloid deposition using PET imaging. *Neurology*. 2020;95(11):e1538-e1553. doi:10.1212/WNL.0000000000010256

3. Braak H, Braak E. Neuropathological stageing of Alzheimer-related changes. *Acta Neuropathol*. 1991;82(4):239-259. doi:10.1007/BF00308809

4. Braak H, Alafuzoff I, Arzberger T, Kretzschmar H, Del Tredici K. Staging of Alzheimer disease-associated neurofibrillary pathology using paraffin sections and immunocytochemistry. *Acta Neuropathol*. 2006;112(4):389-404. doi:10.1007/s00401-006-0127-z

5. Hsu CW, Chang CC, Lin CJ. A Practical Guide to Support Vector Classification. Published online 2003. https://www.csie.ntu.edu.tw/~cjlin/papers/guide/guide.pdf

6. Haufe S, Meinecke F, Görgen K, et al. On the interpretation of weight vectors of linear models in multivariate neuroimaging. *NeuroImage*. 2014;87:96-110. doi:10.1016/j.neuroimage.2013.10.067

7. Chen J, Ooi LQR, Tan TWK, et al. Relationship between prediction accuracy and feature importance reliability: An empirical and theoretical study. *Neuroimage*. 2023;274:120115. doi:10.1016/j.neuroimage.2023.120115

8. Klunk WE, Koeppe RA, Price JC, et al. The Centiloid Project: standardizing quantitative amyloid plaque estimation by PET. *Alzheimers Dement*. 2015;11(1):1-15.e1-4. doi:10.1016/j.jalz.2014.07.003

9. Landau SM, Mintun MA, Joshi AD, et al. Amyloid deposition, hypometabolism, and longitudinal cognitive decline. *Annals of Neurology*. 2012;72(4):578-586. doi:10.1002/ana.23650

10. Su Y, Flores S, Wang G, et al. Comparison of Pittsburgh compound B and florbetapir in cross-sectional and longitudinal studies. *Alzheimers Dement (Amst)*. 2019;11:180-190. doi:10.1016/j.dadm.2018.12.008

11. Jack CR, Wiste HJ, Weigand SD, et al. Defining imaging biomarker cut-points for brain aging and Alzheimer's disease. *Alzheimers Dement*. 2017;13(3):205-216. doi:10.1016/j.jalz.2016.08.005

12. Mormino EC, Kluth JT, Madison CM, et al. Episodic memory loss is related to hippocampal-mediated beta-amyloid deposition in elderly subjects. *Brain*. 2009;132(Pt 5):1310-1323. doi:10.1093/brain/awn320

13. Jagust WJ, Landau SM, Shaw LM, et al. Relationships between biomarkers in aging and dementia. *Neurology*. 2009;73(15):1193-1199. doi:10.1212/WNL.0b013e3181bc010c

14. Therriault J, Pascoal TA, Lussier FZ, et al. Biomarker modeling of Alzheimer's disease using PET-based Braak staging. *Nat Aging*. 2022;2(6):526-535. doi:10.1038/s43587-022-00204-0

15. Pascoal TA, Therriault J, Benedet AL, et al. 18F-MK-6240 PET for early and late detection of neurofibrillary tangles. *Brain*. 2020;143(9):2818-2830. doi:10.1093/brain/awaa180